ACS OMEGA

Open Access

http://pubs.acs.org/journal/acsodf

Article

Resource Estimates for Excited-State Calculations of Diarylethenes on Fault-Tolerant Photonic Quantum Computers

Shu Kanno, Takao Kobayashi, Kimberlee Keithley, and Qi Gao*

Cite This: *ACS Omega* 2025, 10, 18332−18337

Read Online

ACCESS | Metrics & More | Article Recommendations | Supporting Information

ABSTRACT: We estimate computational resources for computing excited-state energies of benchmark photochromic molecules of diarylethenes (DAEs) by using quantum phase estimation on photonic devices. The number of T gates, which determines the calculation time, and logical qubits for a simulation are estimated, considering the overhead of fault-tolerant computers. Three DAE molecules of increasing size are examined with active space sizes specified. Quantum resource estimation is conducted via Hamiltonian truncation within an active space of all valence π electrons in all valence bonding π and their antibonding π^* orbitals. For small and medium molecules, complete active space configuration interaction generates reference energies and trial initial states, while for the large molecule, a trial state with perfect overlap with the exact excited state is assumed due to computational constraints. Notably, with 1.02×10^6 resource state generators, computation for the largest molecule with an active space of 22 electrons and 22 orbitals takes 7 h and 54 min. These results provide insights into the computational resources necessary for computing excited states on quantum hardware.

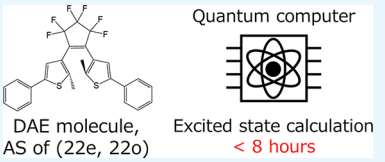

INTRODUCTION

The design and development of advanced electronic and photonic materials are pivotal for driving innovation across various industries,[1−3] including telecommunications, optoelectronics, and renewable energy. Computational methods in quantum chemistry play a central role in accelerating the discovery and optimization of these materials, offering insights into their electronic and optical properties with unprecedented accuracy. Full-configuration interaction (FCI)[4] is the most powerful method for calculating the accurate physical properties of strongly electron-correlated materials with complex electronic structure states and photochemical reactions involving many electronic excited states of various photofunctional materials because FCI can provide exact ground- and excited-state energies within a given basis set. By capturing the interplay between electrons in different orbitals, FCI provides invaluable insights into the ground and excited states of materials, which are essential for understanding their electronic and optical properties. However, traditional computers often struggle to handle large molecular systems due to the exponential scaling of FCI computational resources. This limitation impedes the practical application of FCI to real-world problems, restricting its utility to smaller systems or simplified models.

Quantum computing has emerged as a transformative paradigm in computational chemistry, promising to revolutionize the simulation of molecular systems with unparalleled efficiency and accuracy. The advent of fault-tolerant quantum computers (FTQCs) presents a monumental leap forward, offering the potential to solve practical problems with unprecedented precision.[5] To ensure that future FTQC quantum computers can be applied to FCI calculations and solve practical problems, estimation of the computational resources is essential. By understanding the resource demands upfront, one can assess whether the available hardware and software infrastructure can support the intended simulations. Moreover, by analyzing resource utilization patterns, researchers can devise strategies to enhance algorithm efficiency, reduce computational overhead, and optimize simulation parameters for faster convergence.

In ref 6, the use of quantum phase estimation (QPE) using double-factorized (DF)[7,8] qubitization[9] to compute the ground state of fluoroethylene carbonate was investigated. It presents the analysis of the resource requirements for one of the largest molecules ever considered in quantum computing and develops optimization strategies tailored to the photonic fusion-based quantum computing (FBQC) architecture, utilizing resource state generators (RSGs).[10] An RSG is a photonic device that, every (nanosecond) clock cycle, produces a small, entangled resource state. The results indicated that without further optimization, FBQC could calculate the ground state within a day. However, estimations of excited-state energies are a relatively underexplored area, compared to ground-state energy extractions.

Building on this foundation, our current study extends the approach to estimating the resources required for computing the excited states of diarylethene (DAE) molecules, a class of photochromic materials. DAEs have potential applications in

Received: October 21, 2024
Revised: March 9, 2025
Accepted: April 17, 2025
Published: April 30, 2025

https://doi.org/10.1021/acsomega.4c09568
ACS Omega 2025, 10, 18332−18337

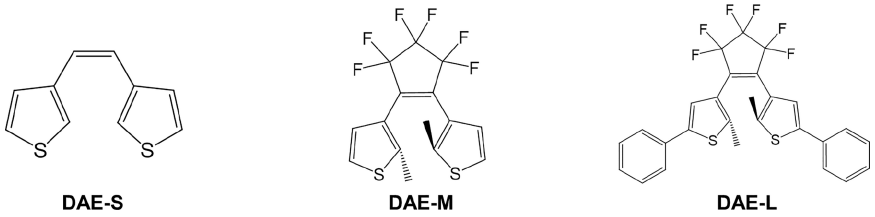

Figure 1. Depiction of the molecules in this study. The left, center, and right molecules are DAE-small, DAE-medium, and DAE-large, respectively.

photoresponsive materials such as single-molecule optical memory, optical switches, and light-driven molecular crystal actuators.[11] In order to rationally design novel DAEs for such applications, it is crucial to calculate the potential energy surfaces (PESs) of electronic ground and excited states involved in the photochromic reaction to high accuracy.

Although PES calculations have so far been performed using quantum chemical methods of time-dependent density functional theory[12,13] and complete active space self-consistent field/CAS second-order perturbation theory with an active space of all valence π electrons in all valence bonding π and their antibonding π^* orbitals,[14] they cannot fully explain experimental results such as the quantum yields (QYs) of the photochromic reactions. For example, in the case of QYs of photochemical ring-opening and closure reactions of DAEs, it is empirically the case that the sum of QYs of photochemical ring-opening and closure reactions is smaller than 1. This mechanism has not been studied by excited-state calculations on classical computers.[11] This indicates that the precise understanding of the photochromic reaction mechanisms of DAEs would require the PESs to be calculated at the level of FCI within the configuration space consisting of all valence electrons in all valence bonding/antibonding/nonbonding orbitals at least, which cannot be realized by conventional classical computers but could be realized by quantum computers.

In this study, as a first step toward FCI calculations of excited states of large-sized DAEs, we estimate the resources and computation time required to calculate DAE excited states at the complete active space configuration interaction (CASCI)[15] level with an active space of all π electrons in all valence bonding π and their antibonding π^* orbitals (22 electrons, 22 orbitals) using QPE on FTQC. The only way to perform such a calculation on classical computers would be to use the density matrix renormalization group,[16−22] which requires heuristic techniques to specify the order and shapes of active orbitals.

METHODS

The estimation procedure is based on a previous work,[6] and thus, we do not show the technical details including quantum circuits and error corrections. We first explain an overview of the estimation and then QPE[23,24], the central quantum algorithm in our estimation, and information to calculate QPE.

Estimation Overview. This work contains baseline resource estimates for computing the excited-state energies of a set of small benchmark DAE molecules via the use of QPE on an FTQC. The goal of such a resource estimate is to determine how long it takes to finish such a computation using a specific number of photonic RSGs, which are the building blocks of the photonic-fusion-based quantum computer. We first determine the number of logical qubits and T gates required to simulate each molecule using a modern qubitization-based approach and factorization of the Hamiltonian, where the number of T gates is an important factor in estimating the computational time. We assume that the hardware operates at a physical error rate equivalent to 10% of the threshold of the error-correcting code.[6] Then, using numerical simulations to determine the required fault-tolerance overhead, we convert these hardware-agnostic quantities into explicit run times and footprints.

QPE and Calculation Details. QPE is a standard and efficient way to sample from the eigenspectrum of a Hamiltonian. QPE takes as input a unitary U and an eigenstate of U, $|\psi_j\rangle$, and outputs an estimate of the corresponding eigenphase ϕ_j in $U|\psi_j\rangle = e^{2\pi i\phi_j}|\psi_j\rangle$ up to some error ϵ, which we can then use to classically compute the eigenenergy $e^{2\pi i\phi_j}$. In particular, we can estimate the electronic eigenenergy of a Fermionic second-quantized Hamiltonian H by taking U to be unitary that encodes a function of the Hamiltonian $f(H)$ and using the eigenstate $|\psi_j\rangle$ to output ϕ_j.

Much of the cost of QPE comes from circuitizing a unitary U that encodes some function of the Hamiltonian $f(H)$. While a popular approach is to approximate the time-evolution[25] unitary e^{-iHt} using product-formula approaches like the Trotter−Suzuki method,[26] we adopt a cheaper approach using *block encoding*[27,28] and *qubitization*,[9] which has led to the most efficient resource estimates for second-quantized simulations of chemistry Hamiltonians.[6−8,29−31]

Since we typically do not have access to the true eigenstate $|\psi_j\rangle$ of the system of interest, we can instead use a trial ansatz state $|\Phi\rangle$ with overlap $\langle\Phi|\psi_j\rangle = \delta$ with the ground state as input to QPE. Because the gate cost of QPE in this study scales with $\lceil\delta^{-1}\rceil$, the calculation time can be minimized by preparing an ansatz with high overlap ($\geq$70%, for example). For molecules of the size considered in this work, there exist sophisticated classical state preparation techniques based on selective configuration interaction approaches where one can use efficiently prepared multideterminant states as initial ansatz to achieve these large overlaps.[32]

We investigate resource estimates for three DAE molecules with varying sizes: (1) a small molecule with 20 atoms, 100 electrons, and 192 basis functions; (2) a medium-sized molecule with 33 atoms, 186 electrons, and 350 basis functions; and (3) a large molecule with 53 atoms, 266 electrons, and 534 basis functions. The structures of the molecules are illustrated in Figure 1. Equal but small active space sizes (10e, 10o) are used for the small- and medium-sized molecules. For the large molecule, an active space of (22e, 22o) is used.

Quantum resource estimation (QRE) is done by Hamiltonian truncation in the above active spaces, and we consider two types of resource-saving techniques, DF and tensor hyper contraction (THC).[8] These techniques use tensor decompositions for electron-repulsion tensors. The cost scales are N^3 for DF and N^2 for THC (where N is the number of basis

https://doi.org/10.1021/acsomega.4c09568
ACS Omega 2025, 10, 18332−18337

functions). While THC first appears to be a more cost-efficient algorithm to use, performing factorization using THC requires performing numerical optimization, which has difficulty with convergence. Molecular orbitals are handpicked for better accuracy for the three lowest singlet states. Reference energies and the trial initial state are generated using the CASCI approach for small- and medium-sized molecules. For the large molecule, CASCI results are inaccessible due to the enormous computational cost on a classical computer, and we assumed that we have access to a trial state that has perfect overlap with the exact excited state and obtained the quantum computational resource needed for an arbitrary excited state.

RESULTS AND DISCUSSION

We first show the results of Hamiltonian generations. Then, we discuss a calculation cost comparison between DF and THC and finally show the improved results by space-time parameter adjustments.

Hamiltonian Generation. We have generated three molecular Hamiltonians, full, DF, and THC, for the molecules DAE-S (small), DAE-M (medium), and DAE-L (large) at the optimized geometries of S_0 transition states (TSs) between closed and open forms, which have biradical characters and were obtained using the broken symmetry spin-unrestricted density functional method of UωB97X with the 6−31G(d) basis set (in which spherical harmonic functions of 5d were used) by Gaussian16.[33] The optimized S_0 TS structures and their corresponding imaginary frequency normal modes are included in the Supporting Information. The CASCI calculations are performed on an active space that consists of all π electrons in all valence bonding π and their antibonding π^* (Hartree−Fock) orbitals. The inputs to the QREs we performed are gathered in Tables 1−3. α in Tables 1 and 2 is

Table 1. Hamiltonians after THC[a]

molecule	R	N_s	α	ERI − ERI^{THC}
DAE-S	55	20	2.3×10^3	5.80×10^{-11}
DAE-M	55	20	4.2×10^3	1.00×10^{-10}
DAE-L	253	44	8.4×10^6	3.90×10^{-8}

[a]N_s is the number of spin molecular orbitals; and ERI is the two-electron repulsion integral. Rank R along with the THC norm is shown. Errors (ERI − ERI^{THC}) are in kcal/mol.

Table 2. Hamiltonians after DF[a]

molecule	threshold	N_s	R	M	α	ERI − ERI^{DF}
DAE-S	1.0×10^{-4}	20	54	480	10.65	0.14
DAE-M	1.0×10^{-4}	20	53	470	10.75	0.15
DAE-L	1.0×10^{-5}	44	207	4080	41.49	0.03

[a]N_s is the number of spin molecular orbitals, the threshold is the cutoff used to truncate the DF Hamiltonian, ERI is the two-electron repulsion integral, R is the maximum rank of terms from DF, and M is the maximum number of eigenvectors for all of the terms from DF. Errors (ERI − ERI^{DF}) are in kcal/mol.

one norm of the approximated Hamiltonian. The error (ERI − ERI^{method}, method = DF or THC) is an l^2 norm between electron-repulsion tensors before and after approximate tensor decompositions.

The errors in THC of Table 1 tend to be smaller than those in DF of Table 2. There are two main explanations for this phenomenon. The first is the trade-off between the error and cost. Obtaining a small error comes at the cost of a larger α compared to that of DF. This causes a large increase in computational cost (see the next section for additional details). The second is the inclusion of nonlinear operations in the optimization step of THC. These nonlinear operations cause errors to suddenly decrease from subkcal/mol to extremely small values during the optimization.

In Table 3, by taking into account the fact that the overlaps δ are close among all of the singlet excited states, we show cost

Table 3. Excited-State Energies and Overlap Assessments from CASCI Results[a]

molecule	excited state	energy	δ	select CASCI	full CASCI
DAE-S	S_0	−1178.24902	0.935	[9, 9]	[252, 252]
DAE-S	S_1	−1178.17469	0.945	[14, 14]	[252, 252]
DAE-S	S_2	−1178.16902	0.928	[25, 25]	[252, 252]
DAE-M	S_0	−1965.38348	0.930	[13, 13]	[252, 252]
DAE-M	S_1	−1965.31294	0.945	[18, 18]	[252, 252]
DAE-M	S_2	−1965.3058	0.928	[24, 24]	[252, 252]

[a]The unit of energy is Hartree; for select CASCI, determinants whose weight is greater than 0.04 are selected. The full/selected CASCI size is represented by the number of alpha and beta spin determinants, amounting to $[\eta_\alpha, \eta_\beta]$, respectively.

estimation results of only S_0 states from the next section. Note that for the large molecule, we assumed that we have access to a trial state that has perfect overlap with the exact excited state since CASCI results are inaccessible due to the enormous computational cost on a classical computer. We show the dependency of weight cutoff on the sum of overlaps and the number of selected determinants in the Supporting Information.

Estimation Results. We discuss the calculation costs of the estimations with the DF and THC. Table 4 shows the result of the comparison between DF and THC. For small and medium molecules, we encountered an unusually large norm for THC. This outcome likely stems from our method's stringent accuracy requirement of ERI − ERI^{method} $\leq$ 0.23 kcal/mol, which may have necessitated retaining the full rank owing to the lack of truncation. The number of T gates per block encoding of THC is significantly smaller than that of DF, which is very promising. However, very high values of α in those cases drive the number of block encodings to be very large, hence making the total cost extremely high. For the large molecule, the THC optimization process did not converge well, and hence, the QREs for the obtained factorization would not give us results with the required precision.

Note that THC achieved high accuracy in the lowered requirements for the problem: namely, less than 2.5 kcal/mol instead of 0.23 kcal/mol. There were no issues with the convergence, and in this case, the resource estimates for THC were orders of magnitude better than those for DF. The results are presented in Table 5.

Cost Improvements. To reduce the calculation cost, we consider adjusting the space-time trade-off parameters. The QREs presented in the previous section have been produced with the parameter $\kappa = 1$ and interleaving length $L = 1$. κ is a parameter for the quantum read-only memory used in DF, and using a higher κ will increase the cost in terms of the number of qubits but will decrease the number of T gates needed to implement this subroutine. L is a parameter for the delay in

https://doi.org/10.1021/acsomega.4c09568
ACS Omega 2025, 10, 18332−18337

Table 4. QRE Results[a]

molecule	method	α	T gates/block	blocks	total T gates	qubit count	time [h]	RSGs
DAE-S	DF	10.65	4.5×10^5	3.3×10^5	1.5×10^{11}	200	0.97	2.9×10^5
DAE-S	THC	2323.37	2.2×10^4	7.3×10^7	1.6×10^{12}	122	10.73	2.2×10^5
DAE-M	DF	10.75	4.4×10^5	3.4×10^5	1.5×10^{11}	200	0.94	2.9×10^5
DAE-M	THC	4198.95	2.2×10^4	1.3×10^8	2.9×10^{12}	122	19.39	2.2×10^5
DAE-L	DF	41.49	1.3×10^7	6.5×10^5	9.0×10^{12}	251	62.27	4.0×10^5
DAE-L[b]	THC	42.13	2.5×10^5	6.6×10^5	1.6×10^{11}	162	1.03	2.5×10^5

[a]We show the number of T gates per block encoding, the number of block encodings, total number of T gates, qubit count, time in hours, and RSGs. Factorizations are performed with a desired accuracy of $\mathrm{ERI} - \mathrm{ERI}^{\mathrm{method}} \leq 0.23$ kcal/mol. [b]Not fully converged because the time for the converged result is extremely high due to the large α.

Table 5. Results for QRE with the Rough Threshold[a]

molecule	method	α	T gates/block	blocks	total T gates	qubit count	time [h]	RSGs
DAE-S	DF	10.62	2.2×10^5	3.3×10^5	7.2×10^{10}	196	0.44	2.6×10^5
DAE-S	THC	13.04	2.0×10^4	4.1×10^5	8.1×10^9	121	0.05	1.8×10^5
DAE-M	DF	10.72	2.1×10^5	3.4×10^5	7.0×10^{10}	196	0.43	2.9×10^5
DAE-M	THC	20.82	2.0×10^4	6.5×10^5	1.3×10^{10}	121	0.08	1.8×10^5
DAE-L	DF	41.36	4.0×10^6	6.5×10^5	2.6×10^{12}	245	18.21	3.9×10^5
DAE-L	THC	37.06	1.4×10^5	5.8×10^5	8.1×10^{10}	162	0.49	2.5×10^5

[a]We show the number of T gates per block encoding, the number of block encodings, total number of T gates, qubit count, time in hours, and RSGs. Factorizations are performed with a desired accuracy of $\mathrm{ERI} - \mathrm{ERI}^{\mathrm{method}} \leq 2.5$ kcal/mol.

Table 6. Improved Results for the QRE[a]

molecule	T gates per block	blocks	total T gates	qubits	time ($L = 1$)	RSGs ($L = 1$)	time ($L = 32$)	RSGs ($L = 32$)
DAE-S	7.1×10^4	3.3×10^5	2.4×10^{10}	629	0.15	6.9×10^5	149	1066
DAE-M	6.9×10^4	3.4×10^5	2.3×10^{10}	629	0.14	6.9×10^5	146	1066
DAE-L	1.7×10^6	6.5×10^5	1.1×10^{12}	743	7.90	1.0×10^6	8088	1362

[a]We chose DF, $L = 1$ and $L = 32$, and $\kappa = 8$. Physical resource counts are given in the number of RSGs, and time is reported in hours, while the algorithm resource count is given in terms of qubit and T-gate counts. The number of T gates required to block encoding the DF Hamiltonian is also included.

optical fibers on a photonic device. Increasing L reduces the number of RSGs but increases the execution times.

We present the results for obtaining the energies of the desired states by changing the parameters. We choose $\kappa = 8$;, at this value, the T-count can be lowered by an order of magnitude with an increase in the number of qubits by about three times. We also adopt $L = 1$ and $L = 32$ to provide a range of potential physical resources needed. The results are presented in Table 6, where we consider only DF with strict accuracy requirements, as in Table 4. The large reduction of time can be found in some conditions. For example, for $L = 1$ in the large molecule, the time is reduced from 62.27 to 7.90 h with 743 logical qubits and 1.0×10^6 RSGs. For $L = 32$, we can reduce RSGs to 10^3, but the computational time is around a year. For DAE-small and DAE-medium molecules, similar computational costs are obtained because both use the same active space size of (10e, 10o) to obtain the truncated Hamiltonian. As a result, we show that we can calculate the excited energy of molecules with classically intractable sizes with a reasonable calculation time under a certain condition by using FTQCs.

CONCLUSIONS

In this work, we explored the quantum computational resources needed to calculate the excited-state energies of three DAE molecules of varying sizes. Leveraging the QPE algorithm, we employed two factorization techniques DF and THC. Through the QRE analysis scheme based on a previous work,[6] we obtained the results that we can calculate classically intractable size molecules in several hours, which depicts the quantum resource requirements under a set of reasonable assumptions on algorithmic choices and hardware parameters. Possible algorithmic improvements could include using an active volume architecture[34] rather than a baseline architecture, doing more research to enable the use of THC for this problem, and improving the core algorithm (e.g., by using Kaiser windows for QPE[35]) and compilation techniques invoked.

Faced with the commercial and scientific value associated with the ability to iteratively explore DAE molecular structure choices to optimize their rational design, we consider this work to be an exciting exploratory step to analyze the role and resources required for FTQCs in this space. In the future, we hope to extrapolate resource demands and predict scalability bottlenecks for larger simulations of practical problems by systematically increasing the size and complexity of the molecular system. We also hope to unlock the full potential of FTQC platforms for advancing scientific discovery and problem-solving in quantum chemistry by accurately assessing resource demands.

ASSOCIATED CONTENT

Supporting Information

The Supporting Information is available free of charge at https://pubs.acs.org/doi/10.1021/acsomega.4c09568.

https://doi.org/10.1021/acsomega.4c09568
ACS Omega 2025, 10, 18332−18337

Calculated S_0 transition state structures and their corresponding imaginary vibrational frequency normal modes for DAE-S, DAE-M, and DAE-L; and overlaps and the number of Slater determinants (PDF)

AUTHOR INFORMATION

Corresponding Author

Qi Gao − *Science & Innovation Center, Mitsubishi Chemical Corporation, Yokohama 227-8502, Japan*; Email: qi.gao.mb@mcgc.com

Authors

Shu Kanno − *Science & Innovation Center, Mitsubishi Chemical Corporation, Yokohama 227-8502, Japan*; orcid.org/0000-0002-8543-8209

Takao Kobayashi − *Science & Innovation Center, Mitsubishi Chemical Corporation, Yokohama 227-8502, Japan*

Kimberlee Keithley − *Science & Innovation Center, Mitsubishi Chemical Corporation, Yokohama 227-8502, Japan*

Complete contact information is available at: https://pubs.acs.org/10.1021/acsomega.4c09568

Notes

The authors declare no competing financial interest.

ACKNOWLEDGMENTS

This work was done with support from PsiQuantum Corp., which implemented the FTQC algorithm and provided the QRE tool as well as valuable inputs. A part of this work was performed for the Council for Science, Technology and Innovation (CSTI), Cross-ministerial Strategic Innovation Promotion Program (SIP), "Promoting the application of advanced quantum technology platforms to social issues"(-Funding agency: QST).

REFERENCES

(1) Committee on Materials Research for Defense After Next; Division on Engineering and Physical Sciences; National Materials Advisory Board; National Research Council, *Materials research to meet 21st century defense needs*; National Academies Press: Washington, D.C., 2003.

(2) Pandikumar, A.; Murugan, C.; Vinoth, S., Eds. *Nanoscale graphitic carbon nitride: Synthesis and applications*; Micro & Nano Technologies; Elsevier Science Publishing: Philadelphia, PA, 2021.

(3) Garnett, E. C.; Ehrler, B.; Polman, A.; Alarcon-Llado, E. Photonics for photovoltaics: Advances and opportunities. *ACS Photonics* **2021**, *8*, 61−70.

(4) Ross, I. G. Calculations of the energy levels of acetylene by the method of antisymmetric molecular orbitals, including σ-π interaction. *Trans. Faraday Soc.* **1952**, *48*, 973.

(5) Shor, P. W. Fault-tolerant quantum computation. *arXiv [quant-ph]* 1996.

(6) Kim, I. H.; Liu, Y.-H.; Pallister, S.; Pol, W.; Roberts, S.; Lee, E. Fault-tolerant resource estimate for quantum chemical simulations: Case study on Li-ion battery electrolyte molecules. *Phys. Rev. Res.* **2022**, *4*, No. 023019.

(7) von Burg, V.; Low, G. H.; Häner, T.; Steiger, D. S.; Reiher, M.; Roetteler, M.; Troyer, M. Quantum computing enhanced computational catalysis. *Phys. Rev. Res.* **2021**, *3*, No. 033055.

(8) Lee, J.; Berry, D. W.; Gidney, C.; Huggins, W. J.; McClean, J. R.; Wiebe, N.; Babbush, R. Even more efficient quantum computations of chemistry through tensor hypercontraction. *PRX Quantum* **2021**, *2*, No. 030305.

(9) Low, G. H.; Chuang, I. L. Hamiltonian simulation by qubitization. *Quantum* **2019**, *3*, 163.

(10) Bartolucci, S.; Birchall, P.; Bombín, H.; Cable, H.; Dawson, C.; Gimeno-Segovia, M.; Johnston, E.; Kieling, K.; Nickerson, N.; Pant, M.; Pastawski, F.; Rudolph, T.; Sparrow, C. Fusion-based quantum computation. *Nat. Commun.* **2023**, *14*, 912.

(11) Irie, M.; Fukaminato, T.; Matsuda, K.; Kobatake, S. Photochromism of diarylethene molecules and crystals: memories, switches, and actuators. *Chem. Rev.* **2014**, *114*, 12174−12277.

(12) Isegawa, M.; Morokuma, K. Photochemical ring opening and closing of three isomers of diarylethene: spin-flip time-dependent density functional study. *J. Phys. Chem. A* **2015**, *119*, 4191−4199.

(13) Xu, D.-H.; Li, L.; Liu, X.-Y.; Cui, G. "On-The-Fly" Non-Adiabatic Dynamics Simulations on Photoinduced Ring-Closing Reaction of a Nucleoside-Based Diarylethene Photoswitch. *Molecules* **2021**, *26*, 2724.

(14) Asano, Y.; Murakami, A.; Kobayashi, T.; Goldberg, A.; Guillaumont, D.; Yabushita, S.; Irie, M.; Nakamura, S. Theoretical study on the photochromic cycloreversion reactions of dithienylethenes; on the role of the conical intersections. *J. Am. Chem. Soc.* **2004**, *126*, 12112−12120.

(15) Gould, M. D.; Chandler, G. S. A unitary group formulation of the complete active space configuration interaction method. I. General formalism. *J. Chem. Phys.* **1989**, *90*, 3680−3685.

(16) Yanai, T.; Kurashige, Y.; Mizukami, W.; Chalupský, J.; Lan, T. N.; Saitow, M. Density matrix renormalization group for *ab initio* Calculations and associated dynamic correlation methods: A review of theory and applications. *Int. J. Quantum Chem.* **2015**, *115*, 283−299.

(17) Yanai, T.; Saitow, M.; Xiong, X.-G.; Chalupský, J.; Kurashige, Y.; Guo, S.; Sharma, S. Multistate complete-active-space second-order perturbation theory based on density matrix renormalization group reference states. *J. Chem. Theory Comput.* **2017**, *13*, 4829−4840.

(18) Lee, S.; et al. Evaluating the evidence for exponential quantum advantage in ground-state quantum chemistry. *Nat. Commun.* **2023**, *14*, 1952.

(19) Chan, G. K.-L.; Sharma, S. The density matrix renormalization group in quantum chemistry. *Annu. Rev. Phys. Chem.* **2011**, *62*, 465−481.

(20) White, S. R.; Martin, R. L. *Ab initio* quantum chemistry using the density matrix renormalization group. *J. Chem. Phys.* **1999**, *110*, 4127−4130.

(21) Sharma, S.; Sivalingam, K.; Neese, F.; Chan, G. K.-L. Low-energy spectrum of iron-sulfur clusters directly from many-particle quantum mechanics. *Nat. Chem.* **2014**, *6*, 927−933.

(22) Baiardi, A.; Reiher, M. The density matrix renormalization group in chemistry and molecular physics: Recent developments and new challenges. *J. Chem. Phys.* **2020**, *152*, No. 040903.

(23) Nielsen, M. A.; Chuang, I. L. *Quantum Computation and Quantum Information: 10th Anniversary ed.*; Cambridge University Press: Cambridge, England, 2010.

(24) Cleve, R.; Ekert, A.; Macchiavello, C.; Mosca, M. Quantum Algorithms Revisited. *arXiv [quant-ph]* 1997

(25) Lloyd, S. Universal quantum simulators. *Science* **1996**, *273*, 1073−1078.

(26) Suzuki, M. Generalized Trotter's formula and systematic approximants of exponential operators and inner derivations with applications to many-body problems. *Commun. Math. Phys.* **1976**, *51*, 183−190.

(27) Gilyén, A.; Su, Y.; Low, G. H.; Wiebe, N. Quantum singular value transformation and beyond: exponential improvements for quantum matrix arithmetics. *Proceedings of the 51st Annual ACM SIGACT Symposium on Theory of Computing*; New York, NY, USA, 2019.

(28) Chakraborty, S.; Gilyén, A.; Jeffery, S. *Power of block-encoded matrix powers: Improved regression techniques via faster Hamiltonian simulation*. 2019; https://drops.dagstuhl.de/entities/document/10.4230/LIPIcs.ICALP.2019.33.

(29) Poulin, D.; Kitaev, A.; Steiger, D. S.; Hastings, M. B.; Troyer, M. Quantum algorithm for spectral measurement with a lower gate count. *Phys. Rev. Lett.* **2018**, *121*, No. 010501.
(30) Berry, D. W.; Kieferová, M.; Scherer, A.; Sanders, Y. R.; Low, G. H.; Wiebe, N.; Gidney, C.; Babbush, R. Improved techniques for preparing eigenstates of fermionic Hamiltonians. *npj Quantum Inf.* **2018**, *4*, 22.
(31) Goings, J. J.; White, A.; Lee, J.; Tautermann, C. S.; Degroote, M.; Gidney, C.; Shiozaki, T.; Babbush, R.; Rubin, N. C. Reliably assessing the electronic structure of cytochrome P450 on today's classical computers and tomorrow's quantum computers. *Proc. Natl. Acad. Sci. U. S. A.* **2022**, *119*, No. e2203533119.
(32) Tubman, N. M.; Mejuto-Zaera, C.; Epstein, J. M.; Hait, D.; Levine, D. S.; Huggins, W.; Jiang, Z.; McClean, J. R.; Babbush, R.; Head-Gordon, M.; Whaley, K. B. Postponing the orthogonality catastrophe: efficient state preparation for electronic structure simulations on quantum devices. *arXiv [quant-ph]* 2018
(33) Frisch, M. J.et al.*Gaussian 1∼6 Revision C.01*; Gaussian, Inc.: Wallingford CT, 2016.
(34) Litinski, D.; Nickerson, N. Active volume: An architecture for efficient fault-tolerant quantum computers with limited non-local connections. *arXiv [quant-ph]* 2022
(35) Greenaway, S.; Pol, W.; Sim, S. A case study against QSVT: assessment of quantum phase estimation improved by signal processing techniques. *arXiv [quant-ph]* 2024

https://doi.org/10.1021/acsomega.4c09568
ACS Omega 2025, 10, 18332−18337